Bollettino di Geofisica Teorica ed Applicata Vol. 59, n. 4, pp. 445-462; December 2018
DOI 10.4430/bgta0250

Modern techniques of treating damage patterns (intensity) to retrieve information on the 6 May 1976 *M* 6.4 earthquake

F. Pettenati, L. Sirovich and D. Sandron

Istituto Nazionale di Oceanografia e di Geofisica Sperimentale - OGS, Trieste, Italy

(Received: 16 February 2018; accepted: 14 September 2018)

ABSTRACT We used all the macroseismic data of the Friuli, 6 May 1976 earthquake to: i) retrieve geometric and kinematic information on the source, by doing automatic nonlinear geophysical inversions; ii) to analyse site effects. The inversions were performed with the KF model of radiation of S body waves in the 10- to 100-km distance range from the source, using a genetic algorithm with niching (NGA). A solution with a N-dipping fault was obtained, with strike angle 266°±10°, dip angle 53°±8°, rake angle 71°±11°. For the site effects we used the type of soil, the depth of the bedrock, the simplified impedance classes and the NEHRP classification. A detailed analysis on the Gemona fan in the epicentral area was also done using intensities from 69 districts of the town. The general analysis confirms amplification on soft soils at great epicentral distances. The analysis of Gemona showed a striking correlation between the trend of macroseismic data and the contour lines of the topography of the fan, with maximum intensity (X-XI, i.e. 10.5) toward the apex of the fan and minimum intensity (VI-VII, i.e. 6.5) in the Friulian Plain beneath it.

Key words: macroseismic intensity, nonlinear geophysical inversion, site effects, Friuli earthquake 1976, seismic response of alluvial fan.

1. Introduction

The Friuli earthquake of 6 May 1976, M_L 6.4 (Slejko *et al*., 1999), M_w 6.45±0.1 (Pondrelli *et al*., 2001) was the most devastating event in north-eastern Italy in the last two centuries (Locati *et al*., 2015). The epicentral area is located in the Friuli - Venezia Giulia (FVG) region, north of the city of Udine. The main shock occurred at 20:00:12 (UTC). In September of the same year, it was followed by four major shocks: 11 September 1976 at 15:31 UTC *M* 5.2, 11 September 1976 at 15:35 UTC *M* 5.6; 15 September 1976 at 02:15 UTC *M* 5.9 and 11 September 1976 at 08:21 UTC *M* 6.0.

In Italy, the main shock struck 77 municipalities, with a death toll of 969 and displacing over 45,000 people from their homes. In the Slovenian area, the damaged municipalities were mainly in the upper and middle valley of the Soča River, especially Bovec, Kobarid and Tolmin. In Austria, the damaged area covered the Kärntnen and Tirol areas. At the time, no local seismographic networks were available. There is, therefore, no unanimous consensus on the source of the earthquake. Various hypotheses from the literature are shown in Fig. 1. In the figure, it can be seen that the proposed seismic sources are distributed in a fairly wide area, from the northernmost ones

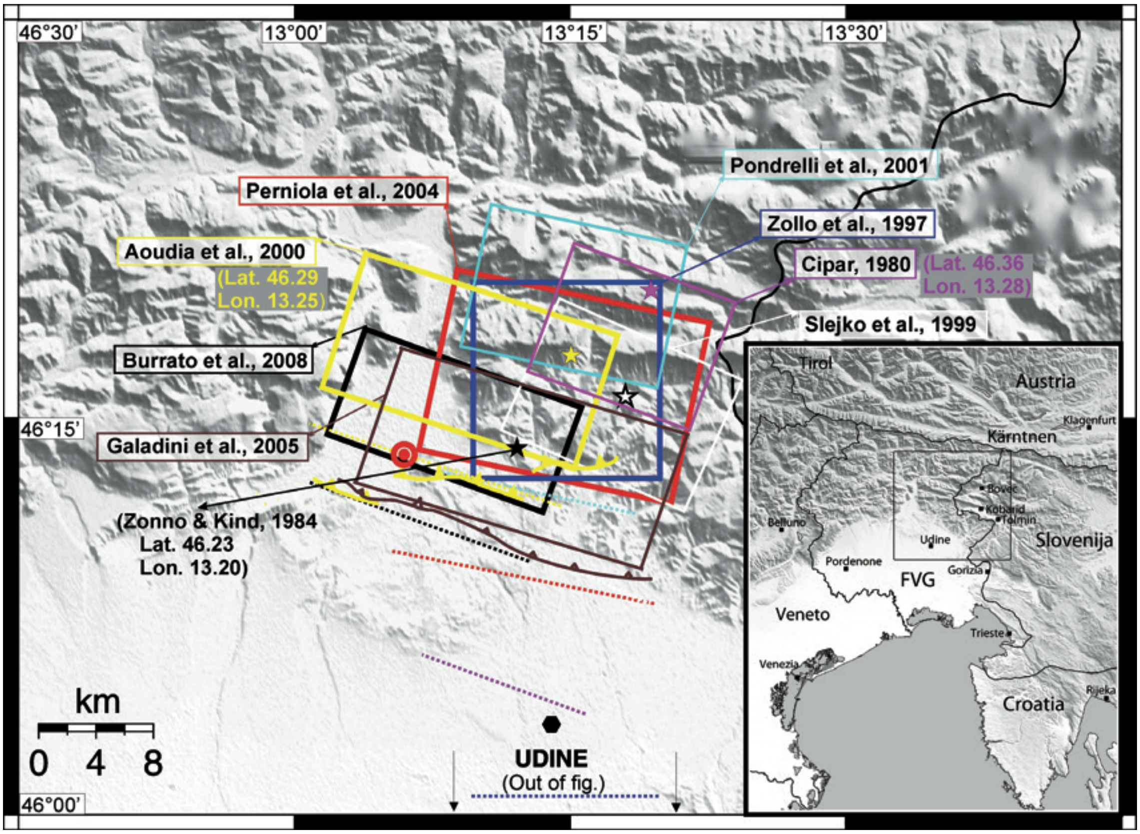

Fig. 1 - Epicentres (stars) and rupture models (rectangles) of the 6 May 1976 main shock and outcrops of geologically active faults in the area, proposed by various authors. Key: magenta Cipar (1980); black Zonno and Kind (1984); yellow Aoudia *et al.* (2000); white Slejko *et al.* (1999); blue Zollo *et al.* (1997); cyan Pondrelli *et al.* (2001); black Burrato *et al.* (2008); brown Galadini *et al.* (2005); red Perniola *et al.* (2004). Double red circle: macroseismic epicentre by Locati *et al.* (2015).

suggested by Cipar (1980) and by Pondrelli *et al.* (2001), to the southernmost models proposed by Galadini *et al.* (2005) and Burrato *et al.* (2008). Apropos, the "ITGG120 Gemona South" source by Burrato *et al.* (2008), is now marked "ITIS120" by the DISS Working Group (2015). The broken segments are their virtual intersections with the topographic surface. The intersection of the model by Zollo *et al.* (1997) is out of the figure. Obviously, it has not been possible to consider that these reverse faults have a concave, listric, shape.

Table 1, summarizes what is depicted in Fig. 1 and some epicentral determination techniques used. One of the first reliable assessments was by Cipar (1980), shared more or less by other authors including the USGS (Anderson and Jackson, 1987), Piromallo and Morelli (1998), Pondrelli *et al.* (2001). Cipar (1980) and Piromallo and Morelli (1998) used body waves (Table 1). More recently, some proposed epicentres were moved further southwards; see the epicentre by Zonno and Kind (1984) in Fig. 1, that was confirmed by Barbano *et al.* (1985) and De Natale *et al.* (1987) (this epicentre was obtained by inverting synthetic seismograms). The hypotheses by Galadini *et al.* (2005) and Burrato *et al.* (2008) are in the southern part of Fig. 1.

In Fig. 1, the rectangular sources drawn with thick lines were proposed by the various authors from their original models. The three rectangles with thin sides (Cipar, 1980; Slejko *et al.*, 1999;

Table 1 - Source parameters of the earthquake of 6 May 1976 in the Friuli region from the literature. The latter alternative consensus model is in brackets, if present.

	Cipar (1980)	**Slejko *et al.* (1999)**	**Aoudia *et al.* (2000)**	**Pondrelli *et al.* (2001)**	**Perniola *et al.* (2004)**	**Galadini *et al.* (2005)**	**Burrato *et al.* (2008)**	**Zollo *et al.* (1997)**	**Anderson and Jackson (1987)**	**Ekström *et al.* (1987)**
M	mb=6 Ms=6.5	Ml=6.4	Ms=6.5	Mw=6.4	Mw=6.4 [a]	M=6.57	Mw=6.4	Ml=6.4	mb=6 Ms=6.5	mb=6 Ms=6.5
Epic. Lat. [°N]	46.36	46.262	46.29	46.36 [b]	46.275 [c]		46.24	46.281 [d]	46.36	46.33
Epic. Lon. [°E]	13.28	13.300	13.25	13.27 [b]	13.246 [c]		13.12	13.256 [d]	13.28	13.17
Prof. [km]	6-10	5.71	7(8.5)	8	6.5			12.9	9	15
Note	Body waves	Stress inversion	Surface waves					Ground acc.		
L [km]	16-20 12	14	18.5	14	18	25	16	13		
W [km]	10 [e]	11 [e]	11.2	11 [e]	14	23	9	13.8		
H [km]			1.5				2-6.5	10		
Strike[°]	76 (290 [h])	88 (294 [h])	288	282 [f]	282 [g]		290	270	76 (267 [h])	284 (74 [h])
Dip[°]	75 (18 [h])	70 (24 [h])	29	23 [f]	23 [g]		30	12	75 (15 [h])	18 (75 [h])
Rake[°]	80 (123 [h])		112	119 [f]	119 [g]	75	105	90	87 (101 [h])	119 (80 [h])
Catalogues	DISS	CFTI	NT4	CPTI						
Epic. Lat. [°N]	46.25	46.233	46.232	46.241 [i]						
Epic. Lon. [°E]	13.14	13.05	13.066	13.119 [i]						

[a] taken from Pondrelli *et al*. (2001);
[b] epicentre almost identical to that by Piromallo *et al*. (1998);
[c] taken from Zonno and Kind (1984);
[d] taken from De Natale *et al*. (1987);
[e] calculated by us using first and third equation of Table 2, page 990, of Wells and Coppersmith (1994);
[f] from Arvidsson and Ekström (1998);
[g] from Pondrelli *et al*. (2001);
[h] auxiliary plane;
[i] obtained using the Boxer algorithm by Gasperini *et al*. (1999);
[l] from instrumental data.

Pondrelli *et al*., 2001) were designed by us for approximate comparison purposes. For this, we used the lengths and widths of the fault planes obtained from the well-known empirical correlations [Table 2 of page 990, first and third equations] of Wells and Coppersmith (1994).

As for the epicentre improvements, the localization of 6 May reported by Peruzza *et al*. (2002) [black circle in their Fig. 1, corresponding to Slejko *et al*. (1999) not shown here] is very close to that of Aoudia *et al*. (2000) [black/white circle in the same figure by Peruzza *et al*. (2002)]. Peruzza *et al*. (2002) used a greater number of replicas than the previous authors. At first, it was thought that the epicentre by Cipar (1980) should be discarded because it was too far north from the aftershocks reported by Aoudia *et al*. (2000); but, when the relocations by Peruzza *et al*. (2002) became available, one understood that it was likely reliable. Aoudia *et al.* (2000) propose an interesting comment: the relocated 34 events along with other aftershocks data located by a

Table 2 - Ranges explored and results of the KF-NGA inversion

Parameters	Range and step	First best fitting	Second solution
Strike angle (°)	0 - 359; 1	266 ± 10	80 (80)[a]
Dip angle (°)	20 - 90; 1	53 ± 8	38 (37)[a]
Rake angle (°) (±180°)	0 - 179; 1	71 ± 11	80 (85)[a]
Nucleation longitude (°)	13.00 - 13.60; 0.01	13.30 ± 0.22	
Nucleation latitude (°)	46.20 - 46.50; 0.01	46.38 ± 0.10	
Depth (km)	4 - 24; 0.1	21.9 ± 3.6	
Rupture length (km) along strike		14.20	
Rupture length (km) anti-strike		11.00	
Vs (km/s)	3.00 - 3.95; 0.01	3.92 ± 0.12	
Mach N. along strike	0.50 - 0.99; 0.01	0.90 ± 0.06	
Mach N. anti-strike	0.50 - 0.99; 0.01	0.80 ± 0.10	
M_0 (10^{18} Nm)	1.0 - 7.0; 1.0	6.9 ± 1.5	
Σr^2		534	555

[h] auxiliary plane of the first best fitting source. We applied one standard deviation as the 68% probability error.

local network and reported in Granet and Hoang (1980) are compatible with the epicentre by Cipar and suggest that the rupture has propagated almost unilaterally toward west. The distribution of aftershocks until August 1976 (Peruzza *et al*., 2002) confirms the presence of some seismicity close to the epicentre by Cipar (1980); therefore, it cannot be discarded for lack of seismic activity in the area. This is, however, compatible with the main part of the rupture being found west and south of the epicentre by Cipar (1980). In Fig. 1, the macrosismic epicentre by Locati *et al*. (2015) is marked by the double red circle SW of the sources proposed, at the opening of the River Tagliamento valley in the Friulian Plain.

Slejko (2018) noticed that two areas remain broadly identified by the previous epicentral determinations: the Resia Valley, NE of Venzone, and the foothills of the Julian Alps, east of Gemona. According to this author, the latter group of locations is more reliable than the former one because it was obtained also by using local stations.

Cipar (1980) calculated one of the first solutions of the focal mechanism (Table 1), but he chose the anti-Alpine plane (dipping south) as the principal plane; the solutions by Anderson and Jackson (1987) and in part also that by Slejko *et al*. (1999) agree with him. On the other hand, Aoudia *et al*. (2000) and Pondrelli *et al*. (2001) chose an Alpine fault source, in accordance with similar sources by Zollo *et al*. (1997) and Burrato *et al*. (2008).

Aoudia *et al*. (2000) believe that a three-piece segmented fault outcropping *en echelon* (Buia, Mt. Bernadia, Susans, drawn in yellow in Fig. 1) could be the superficial prolongation of the causative fault of 6 May, an active structure striking approximately W-E. In Fig. 2, the alignment of the three segments of Aoudia *et al*. (2000) is compatible with the structure indicated by the green arrows (that could also be active according to other authors).

The DISS database (DISS Working Group, 2015) of the Istituto Nazionale di Geofisica e Vulcanologia (INGV) and of Burrato *et al*. (2008) chose the Susans-Tricesimo Fault as a possible fault source in the area [also proposed by Galadini *et al*. (2005)]. In Figs. 2 and 3, this fault is highlighted by the blue arrows. The DISS models by Burrato *et al*. (2008) coincide with the Susans segment, but eastwards the two hypotheses diverge also because Aoudia *et al*. (2000) give credit to an active fault segment along the southern slope of Mount Bernadia. In the section of

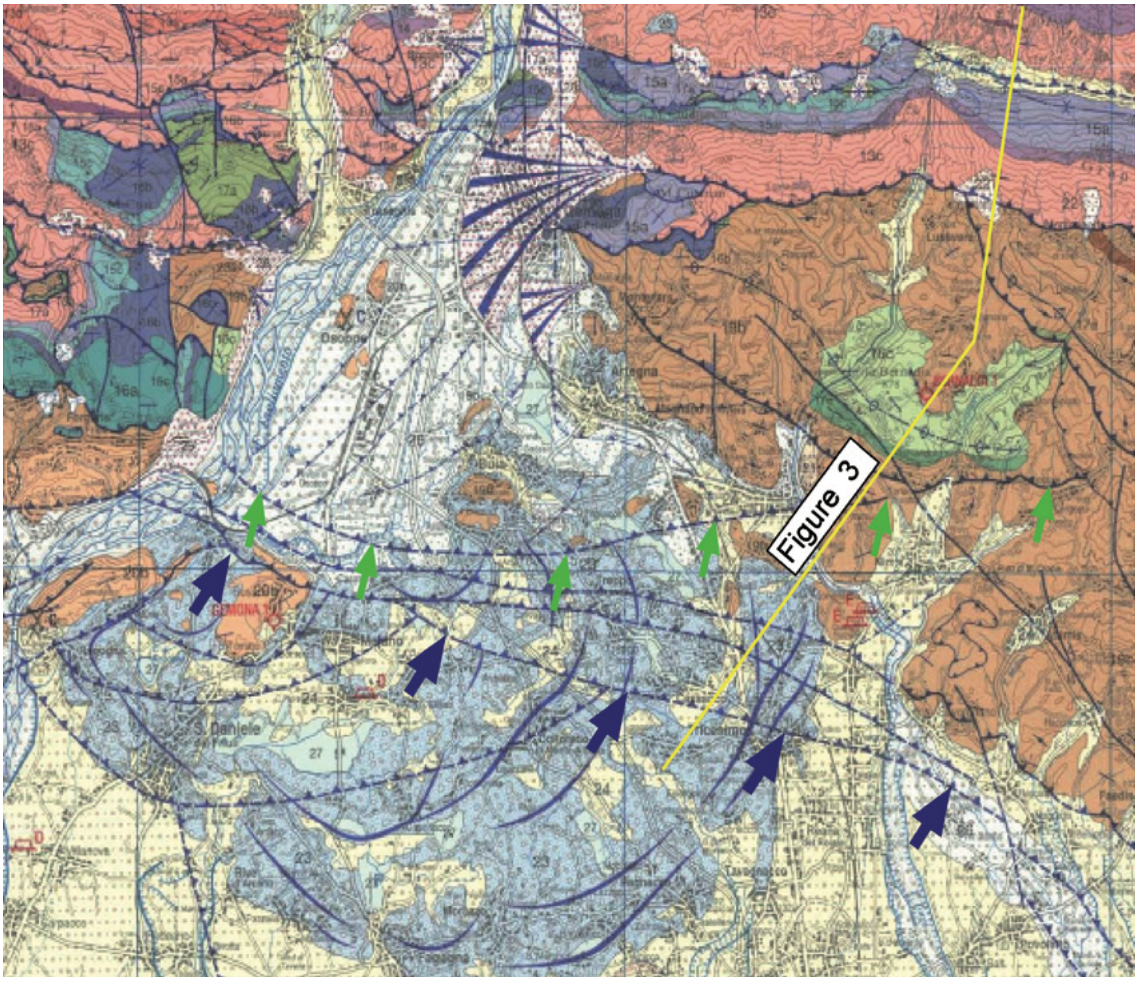

Fig. 2 - Geological map of the study area [extracted and modified from the geological map by Carulli (2006); original scale 1:150,000]. See the trace of the section of Fig. 3. The blue and green arrows point to the outcrops of the two faults highlighted in Fig. 3.

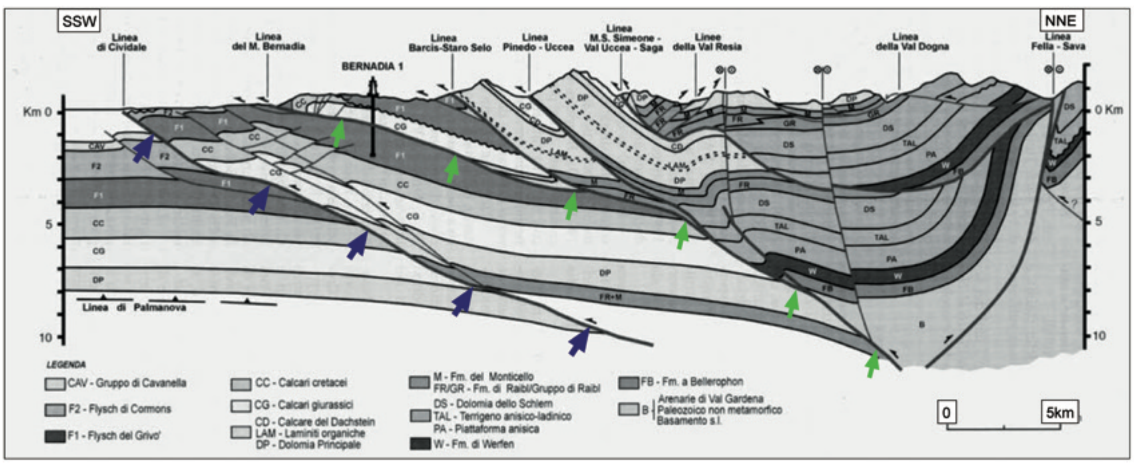

Fig. 3 - Geological section; see the outcrops of two faults in Fig. 2 [modified from Merlini *et al*. (2002)].

Fig. 3, the two structures (Susans-Buia-Mt. Bernadia and Susans-Tricesimo) are identified with the same arrows of Fig. 2.

We are of course aware that there are many reliable fault-plane solutions already available, based on instrumental measurements (see Table 1). From this point of view, this work is an exercise to understand the quality of the solutions provided by the KF-NGA technique in the case of a relatively recent (and well-recorded) earthquake. Then, we also stress that the available intensities presumably contain some site effects (that worsen the inversion). The case study actually compares the solution obtained by KF-NGA inversion with those obtained from various authors who used instrumental data.

In general, the great amount of macrosismic data available for this earthquake gave us the opportunity to test modern methods of treating this type of data. As far as source inversions are concerned, we have previously dealt with such rich data sets with satisfactory results only for the earthquake of Irpinia 1980 [521 data: Sirovich *et al*. (2013)] and that of Calabria in 1905 [453 data: Loreto *et al*. (2012)]. But we have got good inversions, verified on the basis of independent information, even with small sets of data, of 200 and even just 50 data. In the case of the Ferrara earthquake of 1570, we found a reasonable solution in the tectonic context with only 30 point intensities [the found solution explains the deviation of the River Po at the end of the XVI century; Sirovich and Pettenati (2015)].

2. Seismotectonics of the area

In 1976, no coseismic ruptures related to the source faults were detected on the ground. For this reason, the source of 1976 is still controversial. However, it is located in the transition zone between the Southern Alps and the Dinarides. The transition is marked by the Southern Front or Periadriatic Lineament (Placer, 1999; Ponton, 2010), just north of the Adriatic foreland, limited by the Mesozoic margin of the African continental shelf (African microplate). The Periadriatic Lineament is an important tectonic line that runs through this entire Alpine sector tendentially in the E-W direction and has conditioned the geodynamic evolution of this region in the collision between the Adriatic microplate and the European plate since the upper Cretaceous.

As is well-known, in the Southern Alps the tectonic lines have a prevailing E-W direction, dipping northwards, and compressive mechanism, sometimes with a right-hand component (such as the Fella-Sava Line). In the Dinaric region, the tectonic lines are dominated by NW-SE strike and right-hand mechanisms (such as the Ravne and Idrija lines), that accommodate the movement of the Adriatic microplate northwards while subducting under the Southern Alps.

3. Macroseismic data

In May 1976, the collection of information on the macrosismic effects of the earthquake began shortly after the main shock. In December of that year, the first isoseismal map was published by Giorgetti (1976a), at that time in the MSK 1964 scale (Fig. 4). Unfortunately, the article did not report the number of sites investigated and the point intensities, but only the hand-drawn isoseismals; this was the practice of that time, however.

In this article, we used the macroseismic intensity, *I*, data available in 2010 from three catalogues: the Italian one [737 data: catalogue DBMI04 by Stucchi *et al*. (2004)], the Slovenian one by the Agencija Republike Slovenije za okolje, ARSO [210 data: Cecić (2002)] and the Austrian one [946 data: Drimmel *et al*. (1979)]. Tertulliani *et al*. (2018) have re-evaluated the data in the EMS-98 scale. Simplified information on the soil type and thickness is available for many sites. We have thus been able to evaluate if any site effects affect the data set. Eliminated the very low intensities (I = I), 856 intensity points were selected from these three sets within 100 km from the epicentre. Most of the data is on the MCS scale (even the Italian ones); Slovenian ones are in the MSK scale.

There are differences between the two scales, but we preferred not to attempt transformations between different scales; doing so we followed the authoritative opinion of Musson *et al*. (2006): "*intensity values are likely to vary more between two seismologists using the same scale than between two scales used by the same seismologist (at least for twelve-degree scales)*".

Statistical outliers (possible errors, unexplained anomalies, or strong site effects) were sought with the classical Chauvenet method [Barnett and Lewis (1978; pp. 19-20), see also Johnston (1996)], which assumes that the epicentral distances $d(I)$ follow a log-normal distribution, as also in the 1976 data set, among which 23 statistical outliers were found and were, therefore, excluded from the set. The intermediate values, as VI-VII, were rounded to the higher value to respect the concept of macroseismic scales, which have steps corresponding to integer degrees. We believe

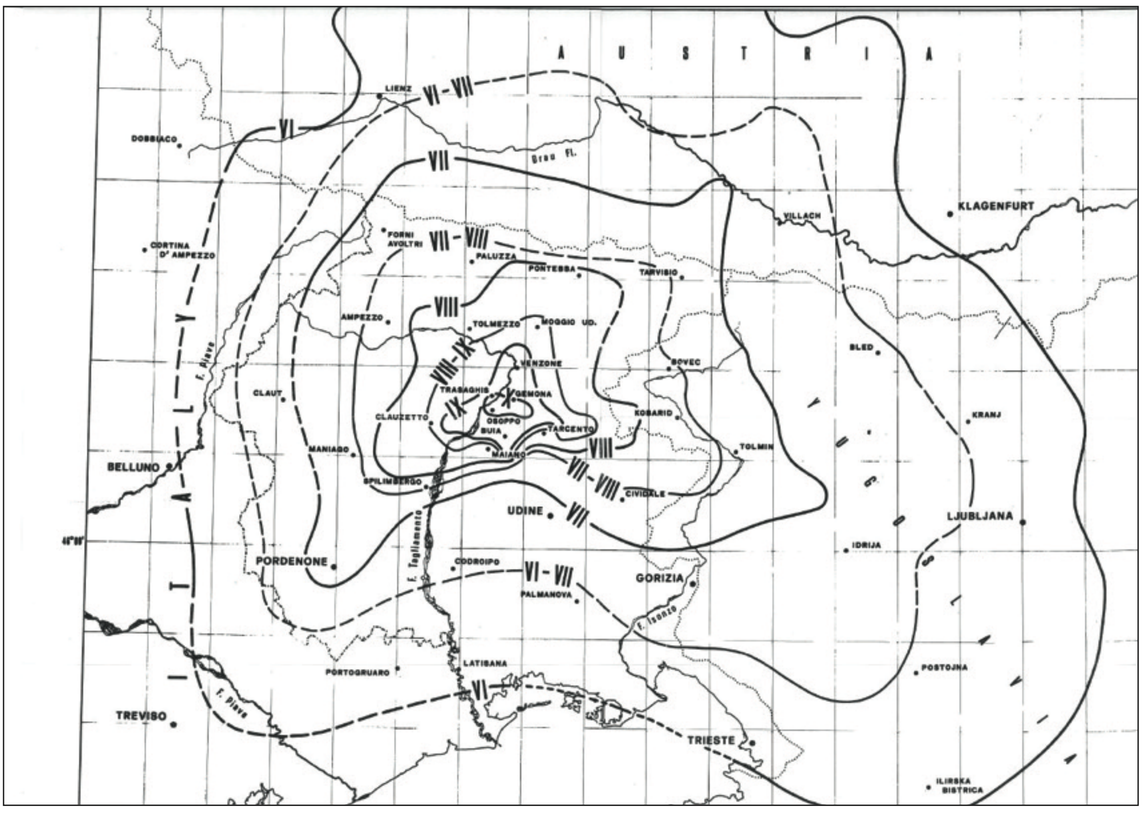

Fig. 4 - Isoseismals of the 6 May 1976 main shock hand-drawn by Giorgetti (1976a) following the practice of the epoch (MSK-64 scale).

that the 1976 data set is of good quality. We drew the isoseismals by contouring the data using the Natural Neighbour algorithm (Sirovich *et al.*, 2002). The result is a picture (Fig. 5a) - obtained without filters or interpretations - quite different from the isoseismals that were hand-drawn in 1976; the figure shows the central part of the surveyed area, between 45.5° and 47.1° latitude, and 12.1° and 14.4° longitude; a total of 833 data was used for this. In Fig. 5a, the isolines pass through the half degrees. Observing Fig. 5, we can see that our contour matches exactly all experimental data. The image shows some anisotropic attenuation, with several small anomalies. Note for example: i) the low radiation southwards, with a large V (blue) area towards the coast; ii) that the IX zone is slightly elongated in the E-W direction, but with a short lobe towards NE and with four *I* = X (purple) islands; iii) that the main isoseismal of *I* = VIII is jagged (ocher colour), with a one degree decrease toward NW that seems to be a minimum of radiation; iv) IV is only reached east and SE (in only 4 sites). Hypothetically, these anomalies could be due to source, path or site effects.

Usually deviations from the surrounding area are of one degree; there are few sites with differences of two degrees. This happens for example - about 25 km ENE of Udine - for two adjacent V degrees (blue) with a small circular crown of VI (pink) in turn included in the VII (yellow) area. At the scale of Fig. 5a, however, it is not possible to hypothesize direct connections between these irregularities and the main physiographic and geomorphological characteristics of the area, shown in Fig. 2. By comparing Figs. 2 and 5a, we refer to the presence of: i) the Friulian Plain in the south and south-western regions of Fig. 5a, ii) the Southern Alps in the northern Italian sector of the figure, iii) the beginning of the Dinaric chain in the Italian and Slovenian eastern sectors of the figure, iv) the eastern Alps in Austria; v) alluvial valleys, sometimes deeply incised, crossing the mountainous areas (such as some parts of the Tagliamento and Fella valleys).

The fact that anomalies greater than one degree are rarely observed, combined with the fact that the *I* data could be affected by uncertainties and evaluation errors, suggests, however, that local effects might have played a minor role in Fig. 5a (we attempted to evaluate site effects however, see the next paragraph).

The likely minor role of site effects is the first reason we have decided not to correct the data. The second is that we do not have univocal policies to make such corrections on all data. The third is that corrections would have left us open to accusations of manipulation. The fourth is that the presence of incorrect data turns into noise in the inversion, but in the previous studies mentiond in the Introduction this has not undermined the results.

The 833 data in Fig. 5a were inverted with the KF-NGA procedure.

4. Searching for site effects

4.1. Searching in the total data set

We performed statistical regressions on *I* data as in Sirovich and Pettenati (2001) and Pettenati and Sirovich (2003). The purpose was to verify the influence of geological site conditions. First, we examined the point data observed in the 219 municipalities of FVG. These 219 data had been associated with simplified geological classifications drawn from the FVG Civil Protection Plan of 2006 (Slejko *et al.*, 2011). The analysis was then extended to 554 FVG sites (Fig. 6). For these 554 sites, the NEHRP classification (Michelini *et al.*, 2008) had also been used but did not show

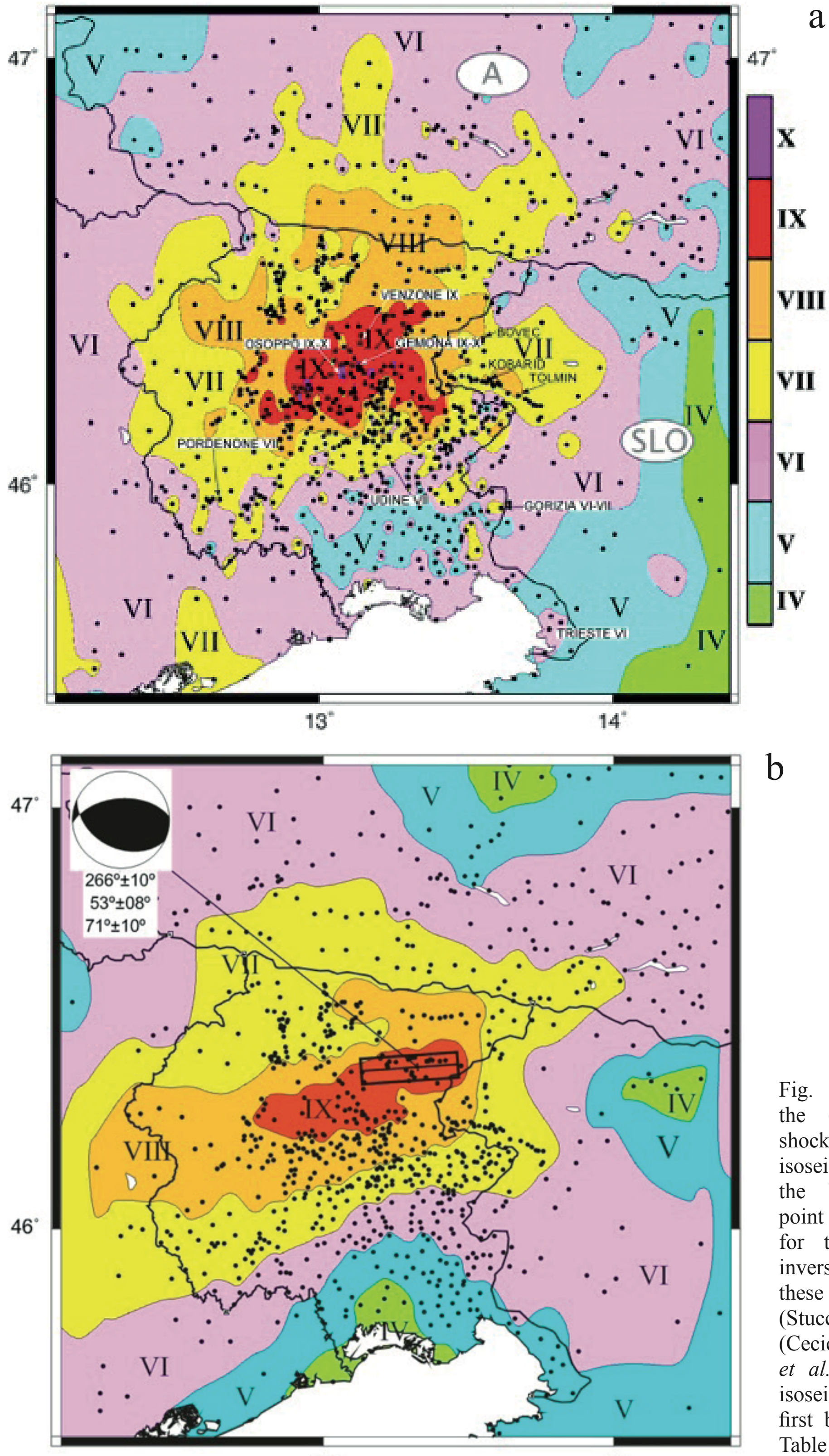

Fig. 5 - Isoseismals of the 6 May 1976 main shock: a) Natural Neighbour isoseismals (see text), the black dots are the point intensities used for the present KF-NGA inversion, they come from these catalogues: DBMI04 (Stucchi *et al.*, 2004); ARSO, (Cecić, 2002); Drimmel *et al.* (1979); b) synthetic isoseismals produced by the first best fitting solution of Table 2, column 3, obtained from our KF-NGA inversion.

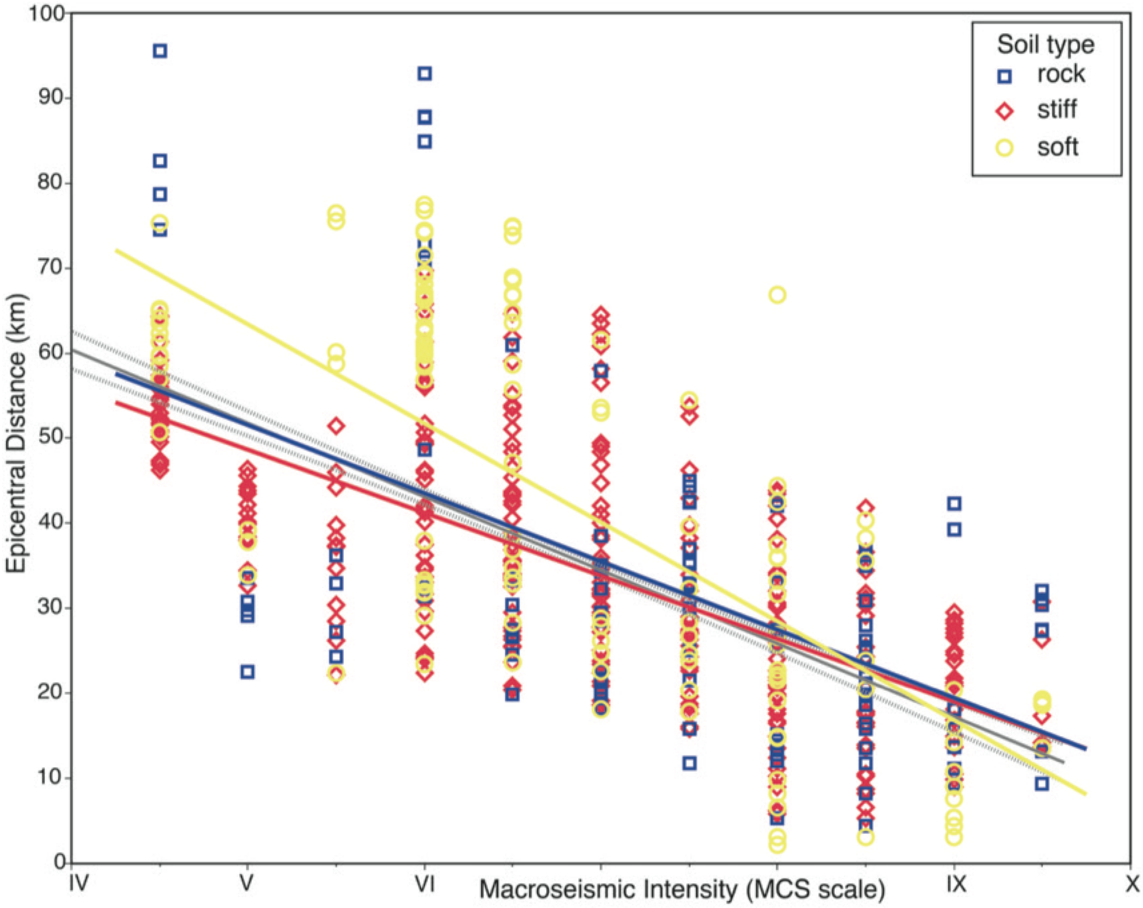

Fig. 6 - Site effects in the 554 sites of the FVG region (Slejko *et al*., 2011). See the text for the key for soft, stiff and rocky sites.

reliable amplification. For the 219 municipalities in the FVG region, we also had approximate information on the depths of the bedrock, but, in this case, the results were statistically unreliable. In Fig. 6, we used the lithologic categories adopted by the R.M.S. Inc., that are described in Pettenati and Sirovich (2003). Fig. 6 shows: the regression line of the total sample (in gray) with the 95% confidence band; soft sites (yellow); stiff (red) and rocky sites (blue). The regressions of Fig. 6 show that soft soils amplify at epicentral distances greater than about 40-50 km. There is a slight tendency for hard ground and rocks to amplify at distances shorter than 15 km, but this clue is unreliable because their regression lines fall within the 95% confidence band of the total sample.

4.2. MSK intensities on the alluvial fan of Gemona

We recovered the original cards of the damage survey for assessing the *I* of 6 May 1976 in the territory of Fig. 7. The figure shows the alluvial fan of the historic centre of Gemona, the slopes of the eastern hills, and part of the plain at the foot of the fan. At the time (the survey begun on 21 May 1976), the cards had been acquired by OGS under the direction of prof. Francesco Giorgetti (Giorgetti, 1976b). The Giorgetti-OGS team had divided the Gemona municipality into 47 built

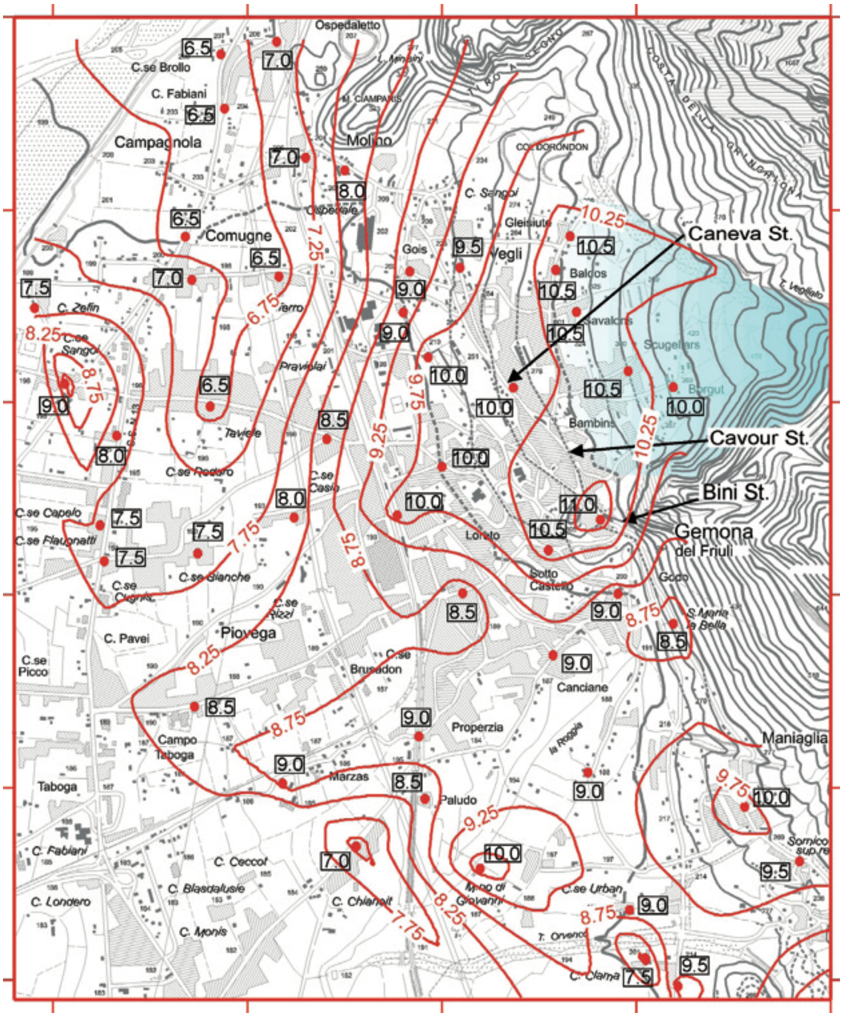

Fig. 7 - Alluvial fan of Gemona, slopes of eastern hills, and part of the plain beneath them. Elevation isolines are in black; Natural Neighbour isoseismals are in red (see text).

areas. It surveyed the damage there and gave the estimated *I* values to the barycentres of the 47 areas. We have positioned these point intensities using a GIS program based on the 1:5,000 scale elements of the current version of the Regional Topography of Friuli-Venezia Giulia. In another layer, however, we also included the scanned paper version of the same type of topography printed in 1974 (1971 flight), i.e. before the earthquake of 6 May 1976. The use of the 1971-1974 topography was indispensable for finding the buildings examined by the Giorgetti-OGS team right after the earthquake.

The red dots in Fig. 7 are the 47 point intensities of the Giorgetti-OGS group; we used the values corrected by hand by prof. Giorgetti in 1976 (†Francesco Giorgetti, 2008, private comunication). The intensities are in the MSK 1964 scale (Medvedev *et al.*, 1965). Thus, Fig. 7 is the only empirical reference available for checking the quality of the simulation of the seismic response of the Gemona fan to the 6 May 1976 earthquake. The contouring of isoseismals in Fig. 7 was performed with the Natural Neighbour technique (Sirovich *et al.*, 2002) on the current digital map (1:25,000 scale; sheet 049-SO Gemona del Friuli). Obviously, the built part seen in Fig. 7 is much wider than in 1971. The highest part of the fan is to the right in Fig. 7. The fan is shaded in blue and the intensity of the colour is proportional to the elevation of the fan with respect to the plain at its foot. In the intensely built areas of Fig. 7, the elevation isolines have been plotted with dashed lines.

Fig. 7 shows two striking features: i) in the area of the fan, the isoseismals are roughly parallel to the elevation contour lines; this suggests an increase in amplification with the increase of the fan thickness; ii) there is a difference of about 3 degrees of *I* between the highest part of the fan and the underlying plain (left in Fig. 7); this is a very high difference in the international case history (the maximum difference of topographic elevation between these two parts is about 160 m).

The isoseismals of Fig. 7 are open to the west, north and east due to the absence of data in those directions. They are, however, closed from SW to the SE thanks to the presence of data in the area of Artegna (outside Fig. 7, but used for the contour).

5. KF inversion

We performed the automatic geophysical inversion of the point intensities of FVG using the KF algorithm with a niching genetic algorithm (NGA). The purpose was to retrieve information on the source. We recall that the KF model treates only body waves (Sirovich, 1996). This technique has already been tested repeatedly by comparing the geometry and kinematics of the causative faults retrieved by KF-NGA inversions with those acquired from modern modelling of instrumental data (in some cases supported by evidence of surface breaks) of a series of recent earthquakes in California (Gentile *et al.*, 2004; Pettenati and Sirovich, 2007). The algorithm has also been tested succesfully with the earthquake of Cansiglio 1936 *M* 6, close to FVG (Sirovich and Pettenati, 2004). In some cases, the KF-NGA source inversions of ancient earthquakes were confirmed by observations of surface fault rupture made by witnesses in the 17th century and found in historical archives (Sirovich *et al*., 2013), and by geomorphological, hydrographic and palaeoseismic data (Sirovich and Pettenati, 2015; Pettenati *et al*., 2017).

In this paper, we use all point intensities (833 data) within 90 km distance from the epicentre, where we suppose that body waves prevail. We are of course aware that there are many reliable fault-plane solutions already available, based on instrumental measurements. We did this exercise especially to understand how the KF-NGA technique behaves in the case of a recent earthquake, with intensities presumably containing some local effects.

We call regression fit the sum of squared residuals Σr^2 (observed-minus-calculated) on the 833 data processed. The best solution has a fit of 534 in Table 2 (column 3). The source of column 3 of Table 2 shows an Alpine style, with a strike nearly E-W (266°±10°), with a dip of (53°±8°) toward the north and a predominantly dip-slip mechanism (Table 2; also see Fig. 5b). As said, the angle of rake (71°±11°) has a strike-slip sinistral component. From the literature, we know of course that the earthquake had a reverse mechanism, but the KF-NGA technique has a ±180° intrinsic ambiguity. The second solution of the inversion (Table 2, column 4) has a fit of 555, strike 80°, dip 38°, rake 80°±180° (we did not calculate its inversion errors). We stress that, when the inverted rake is exactly 90°, there is also perfect ambiguity between the two auxiliary planes. In our case, the rake is 71°, and, then, there is no ambiguity with the auxiliary plane. We comment that the second solution (Table 2, column 4) is, however, not far away from the auxiliary plane of the Alpine fault plane of column 3 of the same table (see Table 2).

6. Discussion

The use of data expressed in different macroseismic scales could have worsened the source inversion (see the relevant errors in Table 2), but did not preclude it. Site effects, therefore, deserve some more discussion, especially because of the peculiar data that we treated (i.e. one *I* value in each town). In general, note that our earlier results suggested that site effects might not have been well preserved in this kind of catalogue in the Los Angeles region and in southern Italy, possibly because towns are often rather far apart and stand in geologically heterogeneous environments (Sirovich and Pettenati, 2001; Pettenati and Sirovich, 2003). We are conscious that the literature offers clear evidence of local *I* amplifications related to town quarters in different geological conditions (which, however, are not reported by the catalogues we use). The results of Fig. 7 confirm that very local site effects can occur, but they are somehow averaged out when the response of the whole town is given by one point *I*. Some observations by Molnar *et al*. (2004) in Greater Victoria for the 2001 Nisqualli earthquake confirm this. In fact, they showed that: 1) the resolutive capacity of the point intensities in a heterogeneous city environment decreased going from street addresses (a full 1.0-unit difference in *I*) to postal code (0.6-unit difference); 2) three-degree differences (as in our Fig. 7) were common on a postal code basis.

The degree of damage to the historical centre of Gemona in 1976 deserves comment. We have also consulted the 1976 damage maps at the municipality of Gemona and performed a survey of the site. We verified that in the centre of the town the buildings of a segment of Bini Street (see Fig. 7) were less damaged than those of neighbouring areas. In this part of Bini Street, the thickness of the alluvial fan would be small and the bedrock almost outcropping; in fact, this site is located along the southern flank of the fan, in the direction of a rocky promontory close to the fan. In Fig. 7 this local drop in intensity cannot be noted because in 1976 the OGS teams observed the damage around the cathedral, and then they moved further NW, bypassing the less damaged section of Bini Street. Giorgetti (1976b) attributed the XI degree (which is likely) to the cathedral area; then, he put four points with $I = 10.5$ towards NNW (Cavour Street towards Caneva Street). However, the aforementioned sampling deficiency of the centre does not affect the result of the three degree amplification between the plain (VII) and the upper part of the fan (X). Note that the point *I* reported for Gemona by the DBMI04 catalogue (Stucchi *et al.*, 2004) is VIII-IX.

Then, as regards site effects on a regional scale, our analysis with regressions and confidence bands confirmed some amplification of soft soils at long epicentral distances.

Coming to the inversion results, the present case study allowed us to compare our solution with those obtained by various authors who used instrumental data. The black rectangle inside the light blue field of Fig. 8 shows the projection of the best fitting solution of Table 2, column 3, for the fault source. The projection was designed using its central values. The light blue field indicates the possible positions of the epicentre identified by the errors reported in the same table. The black thick segment, 11 km long, represents the central value of the length of the line source; on it, the small and thick segment marks the epicentre (the horizontal rupture propagation is almost symmetrical); the thick dashed black segment in Fig. 8 represents the hypothetical intersection of the best fitting solution with the topographic surface (the likely listric shape of the prolongation of the fault in nature is not considered). The large "X" in red, inside the black rectangle, indicates the possible extreme orientations of the line source considering the error of $\pm 10°$ of the strike angle.

The northern line dashed in red (striking WE and almost rectilinear) shows the northernmost theoretical intersection of the prolongation of the best fitting solution with the topographic surface, once the northernmost epicentre and the highest dip angle of the third column of Table 2 are taken into account. The corresponding line dashed in red close to the city of Udine in Fig. 8 has been obtained by considering the errors that move this intersection as far south as possible (the southernmost epicentre and the lowest dip angle). In other words, at the limit of the 95% confidence interval, the theoretical possible outcropping of the fault source would be between the two W-E segments dashed in red (its listric shape not considered).

With respect to Fig. 1, in Fig. 8 we have preserved only the southernmost source found in the literature and the northernmost one; the faults (in yellow) and the macroseismic epicentre are as in Fig. 1. Fig. 8 explains that the best fitting solution of Table 2 is positioned in the northern area of the instrumental sources and that its prolongation (hypothetical plane) would intersect the topographic surface in the zone of the fault segments Susans-Buia-M.te Bernadia and Susans-Tricesimo (in yellow in Figs. 1 and 7). The seismicity reported by Peruzza *et al*. (2002) around the epicentre of Cipar could corroborate our solution.

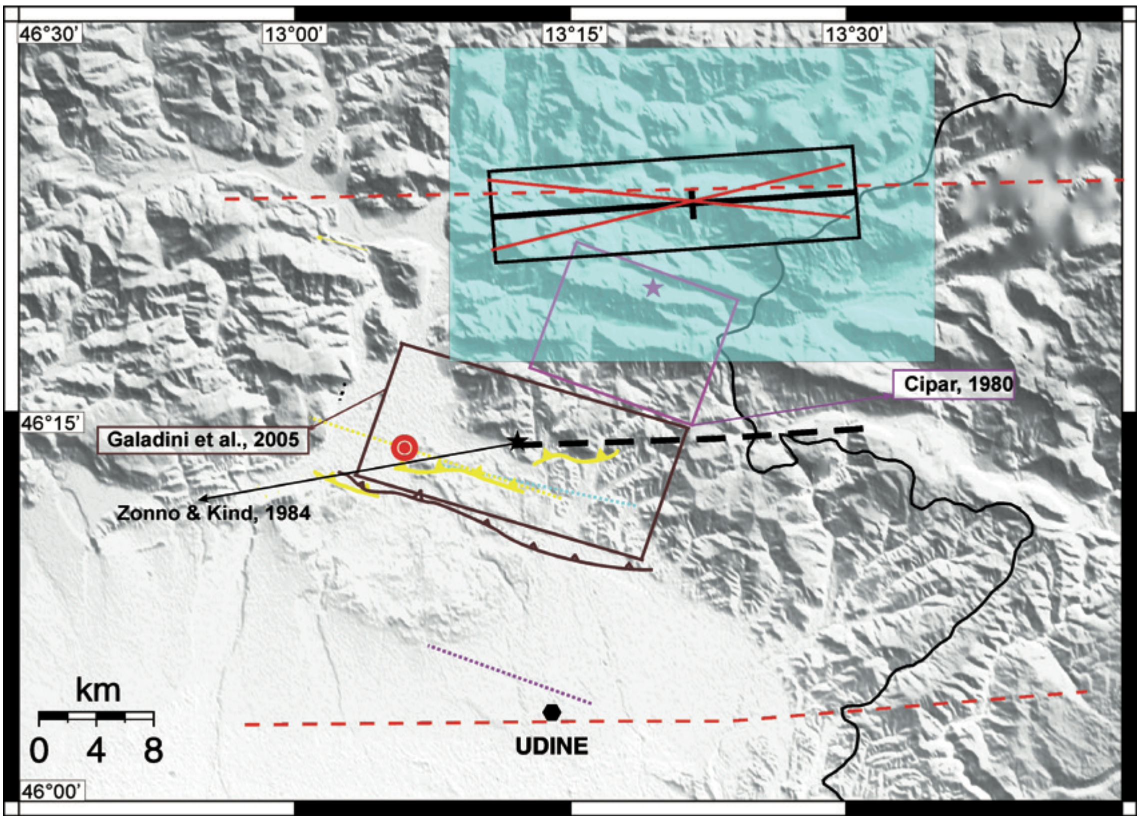

Fig. 8 - The black rectangle is the projection of the best fitting solution (central values) of Table 2, column 3; given the inversion errors in the same table, the epicentre could fall within the light blue field (see the text). The large "X" in red, inside the black rectangle, indicates the possible extreme orientations of the line source considering the error of ± 10° of the strike angle. The southernmost (Galadini et al., 2005) and the northernmost (Cipar, 1980) sources found in the literature are also shown. The thick dashed black segment is the virtual intersection of the best fitting solution with the topographic surface. The northern and southern lines dashed in red are the extreme (virtual) intersections of the best fitting solution with the topographic surface, the epicentral and dip errors considered (see the text).

The hypocentre of Zonno and Kind (1984) is almost 20 km SSW of that of Cipar (1980), but has no fault-plane solution and it is not clear why it is chosen by Burrato *et al*. (2008) to anchor the source "ITGG120 Gemona sud" [now "ITIS120" in DISS Working Group (2015)]. Perhaps it was chosen because it is close to the Susans-Tricesimo structure preferred by those authors. Incidentally, the attributions of earthquakes to faults by Burrato *et al*. (2008) appear to be mostly qualitative; we refer to their tectonically active band coinciding with the foothills from the Aviano Line, to the west, up to the eastern part of Fig. 8. According to them, all strong earthquakes of the catalogue would lie in this band and have thrust mechanisms. This interpretation does not seem exhaustive to us in the Alpine context.

Coming back to the inversion results shown in Table 2, the sinistral rake of our solution (71°±11°) for the plane dipping north is in reasonable agreement only with the values proposed by Galadini *et al*. (2005) (i.e. 75°) and Zollo *et al*. (1997) (i.e. 90°). The values of the rake of the other Alpine solutions, shown in Table 1, are dextral (from 101° to 123°).

The synthetic field of Fig. 5b simulates the observed intensities (Fig. 5a) worse than in other cases inverted so far (e.g. Gentile *et al*., 2004; Pettenati and Sirovich, 2007; Sirovich *et al*., 2013; Pettenati *et al*., 2017). However, the synthetic field shows some interesting features. First, it appears well balanced from *I* IX to IV. Secondly, Fig. 5b reproduces quite well the minimum of the VIII degree of Fig. 5a towards NW. In Fig. 5b there is also a minimum of radiation from VII to IV degree toward east, clearly conditioned by experimental minima VII to V in the same direction in Fig. 5a. Thirdly, the synthetic lobe of IX degree in Fig. 5b reaches the three isolated points of the IX degree west of Osoppo (see Fig. 5a). Towards east, instead, the synthesis of the IX degree is unsatisfactory.

Regarding the seismotectonics of the area, it is worthwile commenting that various authors mentioned in Table 1 chose anti-Alpine solutions. Instead, for many years now there are no doubts that the mainshock of 1976 had an Alpine mechanism. We are glad that the intensity-based KF-NGA technique was able to grasp the Alpine solution. Unfortunately, the *I* data set used herein was made by data points evaluated by different teams using different scales. This brings biases into the observed *I* field and, in turn, changes its shape and brings noise in the whole inversion. On the other hand, the *I* data produced by only one team could be under- or over-estimated, but this would likely bias mostly the length of the inverted source, not its mechanism. Thus, the heterogeneous origin of the *I* data used herein could perhaps explain the large inversion errors in Table 2, which do not allow us to solve the seismotectonic uncertainties summarized in Figs. 2 and 3 (in Table 2, we applied one standard deviation as the 68% probability errors).

7. Conclusions

The data set of the earthquake in question allowed us to test some advances made in treating macroseismic *I* data quantitatively; in particular we tested our KF-NGA technique.

We verified that in the type of macroseismic data used in this paper (one *I* value per each inhabited centre) the site effects seem moderate, perhaps not higher than one degree. We have, however, highlighted that, even using this type of data, it was possible to show that the soft soils amplified at great epicentral distances.

We, then, offer two principal results. First, using the 47 original *I* points produced by the Giorgetti-OGS Group (Giorgetti, 1976b) in Gemona, we clearly identified a striking amplification effect (about three degrees) in the Gemona alluvial fan (Fig. 7). The amplification increases with the topographic altitude, i.e. with the thickness of the alluvial fan sediments.

The second result regards the inversion. If the experiment had been conducted on data from a pre-instrumental earthquake, then the KF-NGA inversion would have allowed at least to: i) place the epicentre approximately in the correct area, and, above all, ii) to understand that the fault had been of Alpine type. In the light of the reference values known from instruments, the other source parameters obtained by our inversion are inaccurate, but not completely wrong. Probably, in the case of Friuli it would be necessary to scale the empirical point *I* data for moderate site effects, but no reliable technique is available for this.

Acknowledgments. Dario Slejko helped us find the correct epicentre in the contradictory presentation by Cipar (1980).

REFERENCES

Anderson H. and Jackson J.; 1987: *Active tectonics of the Adriatic region*. Geophys. J. R. Astr. Soc., **91**, 937-983.

Aoudia A., Saraò A., Bukchin B. and Suhadolc P.; 2000: *The 1976 Friuli (NE Italy) thrust faulting earthquake: a reappraisal 23 years later*. Geophys. Res. Lett., **27**, 573-576.

Arvidsson R. and Ekström G.; 1998: *Global CMT analysis of moderate earthquakes Mw ≥ 4.5, using intermediate period surface waves*. Bull. Seismol. Soc. Am., **88**, 1003-1013.

Barbano M.S., Kind R. and Zonno G.; 1985: *Focal parameters of some Friuli earthquake (1976-1979) using complete theoretical seismograms*. J. Geophys., **58**, 175-182.

Barnett V. and Lewis T.; 1978: *Outliers in statistical data*. John Wiley, Hoboken, NJ, USA, 355 pp.

Burrato P., Poli M.E., Vannoli P., Zanferrari A., Basili R. and Galadini F.; 2008: *Sources of Mw 5+ earthquakes in northeastern Italy and western Slovenia: an updated view based on geological and seismological evidence*. Tectonophys., **453**, 157-176.

Carulli G.B.; 2006: *Carta Geologica del Friuli Venezia Giulia. 1:150.000*. Regione Autonoma Friuli Venezia Giulia, S.E.L.C.A., Firenze, 44 pp.

Cecić I.; 2002: *Potres 6 maja 1976 v Furlaniji: inventarizacija in prevrednotenje makroseizmičkih podatkov za Slovenijo*. ARSO, Ljubljana, Slovenia, Internal report.

Cipar J.; 1980: *Teleseismic observations of the 1976 Friuli, Italy, earthquake sequence*. Bull. Seismol. Soc. Am., **70**, 963-983.

De Natale G., Madariaga R., Scarpa R. and Zollo A.; 1987: *Source parameter analysis from strong motion records of the Friuli, Italy, earthquake sequence (1976-1977)*. Bull. Seismol. Soc. Am., **77**, 1127-1146.

DISS Working Group; 2015: *Database of Individual Seismogenic Sources (DISS), Version 3.2.0: a compilation of potential sources for earthquakes larger than M 5.5 in Italy and surrounding areas*. Istituto Nazionale di Geofisica e Vulcanologia, Roma, Italy, doi: 10.6092/INGV.IT-DISS3.2.0, <diss.rm.ingv.it/diss/>.

Drimmel J., Fiegweil E. and Lukeschitz G.; 1979: *Die auswirkung der Friauler Beben in Österreich*; *makroseismische bearbeitung der starkbeben der jahre 1976/1977 samt historischem rückblick*. Zentralanstalf für Metereologie und Geodynamik, Wien, Austria, Publ. n. 236, 83 pp.

Ekström G., Dziewonski A.M. and Woodhouse J.H.; 1987: *Centroid-moment tensor solutions for the 51 IASPEI selected earthquakes, 1980-1984*. Phys. Earth Planet. Inter., **47**, 62-66.

Galadini F., Poli M.E. and Zanferrari A.; 2005: *Seismogenic sources potentially responsible for earthquakes with M ≥ 6 in the eastern Southern Alps (Thiene-Udine sector, NE Italy)*. Geophys. J. Int., **161**, 739-762.

Gasperini P., Bernardin F., Valensise G. and Boschi E.; 1999: *Defining seismogenic sources from historical felt reports*. Bull. Seismol. Soc. Am., **89**, 94-110.

Gentile F., Pettenati F. and Sirovich L.; 2004: *Validation of the automatic source inversion of the U.S. Geological Survey intensities of the Whittier Narrows, 1987 Earthquake*. Bull. Seismol. Soc. Am., **94**, 1737-1747.

Giorgetti F.; 1976a: *Isoseismal map of the May 6, 1976 Friuli Earthquake*. Boll. Geof. Teor. Appl., **18**, 707-714.

Giorgetti F.; 1976b: *Macroseismic intensity survey by OGS in the Gemona town after the 6 May 1976, M 6.4 Friuli earthquake; 47 damage cards for 47 built areas*. Archive of the Istituto Nazionale di Oceanografia e di Geofisica Sperimentale, Trieste, Italy, <www.ogs.trieste.it/>.

Granet M. and Hoang T.P.; 1980: *Some medium properties at Friuli (Italy) from amplitude spectrum analysis: a possible change in time or in space*. Tectonophys., **68**, 167-182.

Johnston A.C.; 1996: *Seismic moment assessment of earthquakes in stable continental regions: I. Instrumental seismicity*. Geophys. J. Int., **124**, 381-414.

Locati M., Camassi R., Rovida A., Ercolani E., Bernardini F., Castelli V., Caracciolo C.H., Tertulliani A., Rossi A., Azzaro R. and D'Amico S.; 2015: *Database Macrosismico Italiano DBMI15*. Istituto Nazionale di Geofisica e Vulcanologia, Roma, Italy, <emidius.mi.ingv.it/CPTI15-DBMI15/description_DBMI15.htm>.

Loreto M.F., Zgur F., Facchin L., Fracassi U., Pettenati F., Tomini I., Burca G., Diviacco P., Sauli G., Cossarini M., De Vittor C., Sandron D. and the Explora Team of Technicians; 2012: *In search of new imaging for old earthquakes: new geophysical survey offshore Calabria (southern Tyrrhenian sea, Italy)*. Boll. Geof. Teor. Appl., **53**, 385-401, doi:10.4430/bgta0046.

Medvedev S.W., Sponheuer W. and Karnik V.; 1965: *Seismic intensity scale version MSK 1964*. In: Proc. Working Group on Seismicity and Seismo-Tectonics, First Meeting, Tbilisi, Georgia, UNESCO/NS/SEISM/28, 5 pp., 3 tabs.

Merlini S., Doglioni C., Fantoni R. and Ponton M.; 2002: *Analisi strutturale lungo un profilo geologico tra la linea Fella Sava e l'avampaese adriatico (Friuli Venezia Giulia - Italia)*. Mem. Soc. Geol. It., **57**, 293-300.

Michelini A., Faenza L., Lauciani V. and Malagnini L.; 2008: *ShakeMap implementation in Italy*. Seismol. Res. Lett., **79**, 688-697, doi: 10.1785/gssrl.79.5.688.

Molnar S., Cassidy J.F. and Dosso S.E.; 2004: *Comparing intensity variation of the 2001 Nisqually Earthquake with geology in Victoria, British Columbia*. Bull. Seismol. Soc. Am., **94**, 2229-2238.

Musson R., Grünthal G. and Stucchi M.; 2006: *Conversions between older intensity scales and EMS-98*. In: Abstract First European Conference on Earthquake Engineering and Seismology, Geneva, Switzerland, ECEES CD ID542.

Perniola B., Bressan G. and Pondrelli S.; 2004: *Changes in failure stress and stress transfer during the 1976-77 Friuli sequence*. Geophys. J. Int., **156**, 297-306.

Peruzza L., Poli M.E., Rebez A., Renner G., Rogledi S., Slejko D. and Zanferrari A.; 2002: *The 1976-1977 seismic sequence in Friuli: new seismotectonic aspects*. Mem. Soc. Geol. Ital., **57**, 391-400.

Pettenati F. and Sirovich L.; 2003: *Test of source-parameter inversion of the USGS intensities of the Whittier Narrows, 1987 earthquake*. Bull. Seismol. Soc. Am., **93**, 47-60.

Pettenati F. and Sirovich L.; 2007: *Validation of the intensity-based source inversions of three destructive California earthquakes*. Bull. Seismol. Soc. Am., **97**, 1587-1606, doi: 10.1785/0120060169.

Pettenati F., Sirovich L. and Bjerrum L.; 2017: *Fault sources and kinematics of the 1897 Assam (Mw 8.1) and the 1934 Nepal (Ms 8.2) earthquakes retrieved by KF-NGA inversion and their seismotectonic implications*. Bull. Seismol. Soc. Am., **107**, 2480-2489, doi: 10.1785/0120160391.

Piromallo C. and Morelli A.; 1998: *P-wave propagation heterogeneity and earthquake location in the Mediterranean region*. Geophys. J. Int., **135**, 232-254.

Placer L.; 1999: *Contribution to the macrotectonic subdivision of the border region between Southern Alps and External Dinarides*. Geologija, **41**, 223-255.

Pondrelli S., Ekström G. and Morelli A.; 2001: *Seismotectonic re-evaluation of the 1976 Friuli, Italy, seismic sequence*. J. Seismolog., **5**, 73-83.

Ponton M.; 2010: *Architettura delle Alpi Friulane*. Museo Friulano di Storia Naturale, Arti Grafiche Friulane, Imoco di Tavagnacco, Udine, Italy, Pubbl. n. 52, 80 pp.

Sirovich L.; 1996: *A simple algorithm for tracing out synthetic isoseismals*. Bull. Seismol. Soc. Am., **86**, 1019-1027.

Sirovich L. and Pettenati F.; 2001: *Test of source-parameter inversion of the intensities of a 54,000-deaths shock of the seventeenth century in southeast Sicily*. Bull. Seismol. Soc. Am., **91**, 792-811.

Sirovich L. and Pettenati F.; 2004: *Source inversion of intensity patterns of earthquakes: a destructive shock of 1936 in northeast Italy*. J. Geophys. Res., **109**, B10309, doi: 10.1029/2003JB002919.

Sirovich L. and Pettenati F.; 2015: *Source inversion of the 1570 Ferrara earthquake and definitive diversion of the Po River (Italy)*. J. Geophys. Res., **120**, 1-46, doi: 10.1002/2015JB012340.

Sirovich L., Pettenati F., Cavallini F. and Bobbio M.; 2002: *Natural-neighbor isoseismals*. Bull. Seismol. Soc. Am., **92**, 1933-1940.

Sirovich L., Pettenati F. and Cavallini F.; 2013: *Intensity-based source inversion of the destructive earthquake of 1694 in the southern Apennines, Italy*. J. Geophys. Res., **118**, 1-17, doi: 10.1002/2013JB010245.

Slejko D.; 2018: *What science remains of the 1976 Friuli earthquake?* Boll. Geof. Teor. Appl., **59**, 327-350, doi: 10.4430/bgta0224.

Slejko D., Neri G., Orozova I., Renner G. and Wyss M.; 1999: *Stress field in Friuli (NE Italy) from fault plane solutions of activity following the 1976 main shock*. Bull. Seismol. Soc. Am., **89**, 1037-1052.

Slejko D., Carulli G.B., Riuscetti M., Cucchi F., Grimaz S., Rebez A., Accaino F., Affatato A., Biolchi S., Nieto D., Puntel E., Sanò T., Santulin M., Tinivella U. and Zini L.; 2011: *Soil characterization and seismic hazard maps for the Friuli Venezia Giulia region (NE Italy)*. Boll. Geof. Teor. Appl., **52**, 59-104.

Stucchi M., Camassi R., Rovida A., Locati M., Ercolani E., Meletti C., Migliavacca P., Bernardini F. and Azzardo R.; 2004: *Il database delle osservazioni macrosismiche dei terremoti italiani utilizzate per la compilazione del catalogo parametrico CPTI04, DBMI04*. Istituto Nazionale di Geofisica e Vulcanologia, Roma, Italy, <emidius.mi.ingv.it/DBMI04/presentazione.php>.

Tertulliani A., Cecić I., Meurers R., Sović I., Kaiser D., Grünthal G., Pazdírková J., Sira C., Guterch B., Kysel R., Camelbeeck T., Lecocq T. and Szanyi G.; 2018: *The 6 May 1976 Friuli earthquake: re-evaluation and unification of transnational macroseismic data*. Boll. Geof. Teor. Appl., **59**, 417-444, doi: 10.4430/bgta0234.

Wells D.L. and Coppersmith K.J.; 1994: *New empirical relationships among magnitude, rupture length, rupture width, rupture area, and surface displacement*. Bull. Seismol. Soc. Am., **84**, 974-1002.

Zollo A., Bobbio A., Emolo E., Herrero A. and De Natale G.; 1997: *Modelling of ground acceleration in the near source range: the case of 1976, Friuli earthquake (M = 6.5), northern Italy*. J. Seismolog., **1**, 305-319.

Zonno G. and Kind R.; 1984: *Depth determination of north Italian earthquakes using Grafenberg data*. Bull. Seismol. Soc. Am., **74**, 1645-1659.

Corresponding author: Livio Sirovich
Istituto Nazionale di Oceanografia e di Geofisica Sperimentale - OGS
Borgo Grotta Gigante 42c, 34010 Sgonico (TS), Italy
Phone: +39 040 2140249; e-mail: lsirovich@inogs.it